



Published in final edited form as:

*J Nat Prod.* 2011 December 27; 74(12): 2545–2555. doi:10.1021/np200673b.

## Natural Product Libraries to Accelerate the High Throughput Discovery of Therapeutic Leads<sup>‡</sup>

Tyler A. Johnson<sup>†,‡,\*</sup>, Johann Sohn<sup>†</sup>, Wayne D. Inman<sup>‡</sup>, Samarkand A. Estee<sup>‡</sup>, Steven T. Loveridge<sup>‡</sup>, Helene C. Vervoort<sup>‡</sup>, Karen Tenney<sup>‡</sup>, Junke Liu<sup>∇</sup>, Kenny Kean-Hooi Ang<sup>⊥</sup>, Joseline Ratnam<sup>⊥</sup>, Walter M. Bray<sup>§</sup>, Nadine C. Gassner<sup>§</sup>, Young Y. Shen<sup>∇</sup>, R. Scott Lokey<sup>§,‡</sup>, James H. McKerrow<sup>||</sup>, Kyria Boundy-Mills<sup>○</sup>, Arif Nukanto<sup>#</sup>, Atit Kanti<sup>#</sup>, Heddy Julistiono<sup>#</sup>, Leonardus B. S. Kardono<sup>##</sup>, Leonard F. Bjeldanes<sup>†</sup>, and Phillip Crews<sup>‡,\*</sup>

<sup>†</sup>Department of Nutritional Sciences & Toxicology, University of California, Berkeley, California 94720, United States

<sup>‡</sup>Department of Chemistry & Biochemistry, University of California, Santa Cruz, California 95064, United States

<sup>§</sup>UCSC Chemical Screening Center, University of California, Santa Cruz, California 95064, United States

<sup>⊥</sup>Sandler Center for Drug Discovery, University of California, San Francisco, California, 94143, United States

<sup>||</sup>Small Molecule Discovery Center, University of California, San Francisco, California 94158, United States

<sup>∇</sup>Eisai Inc., Natural Product Lead Discovery, Andover, Massachusetts 01810, United States

<sup>○</sup>Phaff Yeast Culture Collection, Food Science and Technology, University of California Davis, Davis California 95616, United States

<sup>#</sup>Research Center for Biology, Indonesian Institute of Science (LIPI), Cibinong, 16911

<sup>##</sup>Indonesia & Research Center for Chemistry, Indonesian Institute of Science (LIPI), Serpong, Tangerang 15310, Indonesia

### Abstract

A high throughput (HT) paradigm generating LC-MS-UV-ELSD based natural product libraries to discover compounds with new bioactivities and or molecular structures is presented. To validate this methodology an extract of the Indo Pacific marine sponge *Cacospongia mycofijiensis* was evaluated using assays involving cytoskeletal profiling, tumor cell lines, and parasites. Twelve known compounds were identified including the latrunculins (**1–4**, **10**), fijianolides (**5**, **8–9**), mycothiazole (**11**), the aignopsanes (**6–7**) and sacrotride A (**13**). Compounds **1–4**, **5**, **8–11** exhibited bioactivity not previously reported against the parasite *T. brucei*, while **11** showed selectivity for lymphoma (U937) tumor cell lines. Four new compounds were also discovered including: aignopsanoic acid B (**13**), apo latrunculin T (**14**), 20-methoxy-fijianolide A (**15**) and aignopsane ketal (**16**). Compounds **13** and **16** represent important derivatives of the aignopsane

\*To whom correspondence should be addressed. Tel: (831) 459-4280. taj\_uch@berkeley.edu. Tel: (831) 459-2603. pcrews@ucsc.edu.

<sup>‡</sup>Dedicated to Professor Joseph F. Bunnett on the occasion of his 90<sup>th</sup> Birthday.

**Supporting Information Available.** Four tables and 53 figures are provided. These data include the <sup>1</sup>H NMR spectra for compounds **1–13** and **17–19** along with 1D and 2D NMR spectra for compounds **14–16**, bioassay data for **18–19**, an instrumentation diagram for the LC-MS-UV-ELSD library setup and demonstrations of how to weigh removable 96 well plate libraries including a sample workup sheet. This material is available free of charge via the Internet at <http://pubs.acs.org>.

class, **14** exhibited inhibition of *T. brucei* without disrupting microfilament assembly and **15** demonstrated modest microtubule stabilizing effects. The use of removable well plate libraries to avoid false positives from extracts enriched with only 1–2 major metabolites is also discussed. Overall, these results highlight the advantages of applying modern methods in natural products-based research to accelerate the HT discovery of therapeutic leads and or new molecular structures using LC-MS-UV-ELSD based libraries.

---

The role of natural products or their derivatives as tools in developmental therapeutics programs has been substantial.<sup>1–4</sup> However, despite a sustained record of important contributions, during the last 15 years there has been a de-emphasis especially by the biopharmaceutical industry in natural products-based discovery programs.<sup>5</sup> A major reason cited for dropping early stage natural products discovery programs includes the lengthy time scales involved in the bioassay guided pursuit to identify or dereplicate potential new lead compounds.<sup>6</sup> Skepticism has also been expressed about the prospects in designing effective natural products-based platforms that would incorporate modern high throughput screening (HTS).<sup>5</sup>

There has been a precipitous decrease in new molecular entity (NME) approved drugs by the US Food and Drug Administration (FDA) over the last 20 years. For example, the count of 45 agents approved in 1990 decreased to 21 in 2010.<sup>1, 7</sup> In our view, there appears to be a positive correlation with the diminished focus on natural products as sources of new therapeutic leads and the drop in the number of NME approved drugs. Whether these trends are causal or coincidental is open to debate, but few would disagree on the significant role of natural products in providing sources and inspiration for new therapeutic leads.<sup>8</sup> One bright spot amidst this controversy is that interest in natural products-based discovery programs in the developing world has increased dramatically since the adoption of the Convention on Biological Diversity (CBD) in 1993.<sup>6</sup> As another development, several companies engaged in natural products research including Sequoia Sciences,<sup>9</sup> AnalytiCon Discovery,<sup>10</sup> and Wyeth<sup>11</sup> plus a small number of academic groups have published first generation results showing that high throughput (HT) HPLC purification methods can be interfaced with modern HTS bioassays.<sup>12–15</sup> Surprisingly, only a few studies of this type from academic groups have taken the next step involving the use of such HT approaches culminating in the disclosure of compounds with completely new biological activities or molecular structures.<sup>13–17</sup> As one exception, the UC Santa Cruz consortium has recently revealed that combining HT HPLC methods with a HT Yeast Halo assay successfully pinpointed the unreported anti-fungal bioactivity of crambescidin 800.<sup>14</sup> We have now further optimized this strategy to identify lead compounds through an approach that incorporates systematic LC-MS-UV-ELSD analysis. The impetus for these changes stemmed from partnerships developed in a multi-disciplinary campaign as part of a natural products-based International Cooperative Biodiversity Group (ICBG)<sup>6</sup> initiative. We have formed a powerful alliance, which involves contributions from Indonesian professionals working alongside investigators from four University of California campuses.

A key tool introduced to guide our ICBG programs consists of a refined HT screening paradigm. The goal is to accelerate identifying compounds with unreported bioactivity and or new structures and it involves the four step process outlined in Scheme 1. 1) Raw materials, which can vary from marine sponges, tropical plants, or culture broths from microorganisms, are pre-fractionated using traditional methods<sup>18</sup> or with our previously described HT approach of accelerated solvent extraction (ASE)<sup>19</sup> which reduces the extraction cycle times from hours/days to minutes. This creates semi-crude extract assortments (SCEAs), and only the MeOH plant extracts are further pre-treated in the first step using solid phase extraction (SPE) cartridges, to remove polyphenols, which can act as

false bioassay positives.<sup>12</sup> 2) The SCEAs are evaluated in a panel of HT bioassays<sup>20</sup> involving cytoskeleton activity,<sup>21</sup> immune modulation,<sup>18</sup> parasites,<sup>22</sup> tumor cell lines<sup>18, 23</sup> and opioid receptors.<sup>24</sup> 3) Prioritized active extracts are then selected for LC-MS-UV-ELSD library creation into 96 well plates with subsequent follow up HT bioassay evaluation. 4) When fractions (containing potential lead compounds) that either exceed the potency of the SCEAs or possess new  $m/z$  values are identified, further processing is immediately initiated. This involves using the same column and LC-MS-UV-ELSD conditions of step 3 to scale up into 20 mL vials (or 50 mL test tubes), followed by evaporation, NMR, dereplication and or structure elucidation. This protocol addresses several key HT parameters<sup>11, 25</sup> including: a) modest expense accompanied by an easy setup and implementation, b) minimal volumes of solvent are required to process ASE extracts,<sup>19</sup> 96 well plate, or 20 mL vial scale up fractions, c) nuisance substances (e.g. salts or polyphenols) that can interfere with bioassays are effectively removed, d) the rapid processing provides high quality purification followed by concentration of lead compounds into a library for direct HTS bioassay, and e) frontline acquisition LC-MS  $m/z$  ion, UV and ELSD data analysis serves to jumpstart dereplication and structure elucidation efforts.

We implemented the process outlined in Scheme 1 to test the hypothesis that using a focused HT strategy would provide rapid identification of lead compounds with important activity properties and the discovery of new compounds from even well studied species. The proof of concept trial involved investigation of individual specimens of the Indo Pacific sponge *Cacospongia mycofijiensis*. Extracts of this sponge have been the source of seven major structural classes having various forms of bioactivity, some with unique mechanisms of action. The structures include: the latrunculins (anti-tumor, microfilament disruption),<sup>26, 27</sup> fijianolides (syn laulimalide, anti-tumor, microtubule stabilizing),<sup>28, 29</sup> dendrolasen (cytotoxic, target unknown),<sup>30</sup> mycothiazole (solid tumor selective, mitochondria complex I),<sup>31, 32</sup> dactylolide (cytotoxic, microtubule stabilizing),<sup>33</sup> CTP-431 (cytotoxic, target unknown)<sup>34</sup> and the aignopsanes (moderate anti-parasitic, mechanism unknown).<sup>35</sup> The results of our HT survey of *C. mycofijiensis* plus additional insights discovered during our brief evaluation using LC-MS-UV-ELSD of other assemblages are discussed below.

## Results and Discussion

A 2007 Papua New Guinea collection of *C. mycofijiensis* (coll. no. 07327) composed of 15 individual specimens (subtypes **A-0**, see Figure S1; S denotes Supporting Information) were extracted using an accelerated solvent extractor (ASE, denoted as X)<sup>19</sup> and the  $\text{CH}_2\text{Cl}_2$  extracts (samples coded as FD) were profiled for chemical diversity using LC-MS-UV-ELSD (see Figures S2–S4). The sponge colony, sample 07327 **F** XFD, displayed the most complex LC trace (see Figure 1a) and  $^1\text{H}$  NMR spectra (see Figure S5); and it was selected for screening using the assays in Table 1 (entry 1). This extract showed broad spectrum bioactivity including: a) microfilament (MF) disruption and microtubule (MT) stabilizing effects, and b) low  $\mu\text{g/mL}$  inhibition against the parasite *Trypanosoma brucei* and/or against several tumor cell lines. In an effort to quickly identify the compound(s) responsible for the activity an LC-MS-UV-ELSD library shown in Figure 1b was generated and shuttled to three institutions for evaluation, followed by automated scale up HPLC. Shown in Figure 2 are 11 known compounds with unreported biological activity that were de-replicated alongside four new compounds and one known compound unreported from this species.

The next task was to correlate the activity of the parent extract XFD (Table 1) with that of specific compounds by evaluating the LC-MS and NMR data of selective library fractions. A small subset of fractions were active in the MF and MT or both assays. The entries 2, 4, 7 and 12 in Table 1 displayed MF disrupting effects at 20  $\mu\text{g/mL}$ . The LC-MS  $m/z$  data in Table 1 and  $^1\text{H}$  NMR (see Figures S6–S9, S15) of these fractions, plus entry 3, all

corresponded to the latrunculin A (**10**) chemotypes (**1–4**).<sup>27</sup> Not surprisingly, entries 8, 10–11 and 14 exhibited microtubule stabilizing effects at 20 µg/mL with *m/z* values and <sup>1</sup>H NMR data in agreement with the fijianolides (**5**, **8–9**, see Figures S10, S13–S14).<sup>28</sup> The <sup>1</sup>H NMR (see Figure S33) and microtubule stabilizing effects of entry 14 (Fraction H57, 513 *m/z*) was similar but did not match any previously reported fijianolides<sup>28, 36</sup> and it was set aside for further characterization.

All 17 fractions listed in Table 1 were evaluated against *T. brucei*, the parasite responsible for Human African trypanosomiasis (HAT).<sup>22</sup> Only six of the samples (entries 2, 7, 8, 10, 11, 12) demonstrated good inhibitory activity (~1 µg/mL) and these contained the latrunculins (**1**, **4**, **10**)<sup>27</sup> and fijianolides (**5**, **8–9**).<sup>28</sup> Less potent were five fractions (entries 3, 4, 6, 9, 13) which also showed modest inhibition (< 10 µg/mL), and the active constituents contained the latrunculins (**2**, **3**, **14**)<sup>27</sup>, an aignopsane (**6**)<sup>35</sup> and mycothiazole (**11**)<sup>31</sup>. The values of the first set are on par with natural products investigated by others<sup>37</sup> and are less potent than the clinically used but broadly cytotoxic agent melarsoprol (IC<sub>50</sub> = 0.0026 µM).<sup>38</sup> The LC-MS *m/z* ions of the various fractions were used to pinpoint the presence of these compounds and most were confirmed (i.e., see Figures S11, S16). The exceptions to this analysis included the following: the LC-MS *m/z* ion (404 amu) and <sup>1</sup>H NMR data (see Figure S27) of entry 6 resembled latrunculin A (**10**), but were not an exact match. The LC-MS *m/z* ion (513 amu) and <sup>1</sup>H NMR data (see Figure S33) of entry 14 also did not match that of previously described compounds. Thus, this material was added to the list of compounds needing additional analysis. Some further noteworthy points pertaining to the more bioactive compounds in this group are as follows. The compound latrunculol A (**1**) is being pursued as a preclinical anti-tumor candidate<sup>39</sup> due to its selective cytotoxicity for colon cancer (C38) vs normal bone marrow (CFU-GM) cell lines.<sup>27</sup> Other latrunculin analogs have also recently emerged as potential anti-tumor, anti-microbial, anti-fungal, and anti-protozoal therapeutic leads.<sup>27, 40–43</sup>

The final analysis involved assaying the library fractions against solid tumor cell lines including melanoma (MDA-MB-435), colon (HT-29), non small cell lung (H522-T1) and lymphoma (U937). Considerable cytotoxicity (< 2.5 µg/mL) was observed for the parent extract, entry 1 as well as for library fractions, entries 2, 7, 10–13. These active constituents corresponded to compounds **1**, **4**, **8–11** and similar results have been reported previously.<sup>27, 28, 31, 44</sup> Although **1**, **4**, **8–10** were roughly equally active in the assays, mycothiazole (**11**) showed distinct solid tumor selectivity for U937 cells (0.01 µg/mL) versus MDA-MB-435 (1.0 µg/mL), HT-29 (0.7 µg/mL) and H522-T1 (1.0 µg/mL) cell lines. Compound **11** has previously shown selectivity in the NCI panel of 60 cell lines,<sup>31</sup> but data for U937 has not been reported. These results highlight the utility of using this HT approach to identify lead compounds with unreported selectivity for additional cancer cell lines.

The compositions of four other fractions (entries 5, 15–17) were also investigated based on their unique LC-MS and <sup>1</sup>H NMR data. Entry 5 (Fraction H30, 269 *m/z*) gave a <sup>1</sup>H NMR spectrum (see Figure S18) similar to the aignopsanes<sup>35</sup> but lacked a UV chromophore, and was visible only by ELSD. It was designated for further structure elucidation work. Entry 15 (Fraction H59, 265 *m/z*) had LC-MS and <sup>1</sup>H NMR data (see Figure S12) identical to methyl aignopsanoate **7**.<sup>35</sup> Entry 16 (Fraction H61, 249 *m/z*) was identified as discussed below as the ketal derivative of **6** based on <sup>1</sup>H NMR (see Figure S39). Entry 17 (Fraction H65, 463 *m/z*) was also only visible by ELSD. Its LC-MS *m/z* and NMR spectroscopic data (see Figure S17) matched that of sacrotride A (**12**),<sup>45</sup> a common bioactive compound from sponges,<sup>46</sup> but unreported from this species.

At this point it was clear that four new compounds were present in the fractions (entries 5–6, 14, 16), which also exhibited LC-MS *m/z*, NMR and or bioactivity data not previously

reported from *C. mycofijiensis*. The first to be analyzed was entry 5 (Fraction H30, 269  $m/z$ ) which had a metabolite whose molecular formula of  $C_{15}H_{24}O_4$  from HRESITOFMS was based on the  $[M+Na]^+$  ion  $m/z$  291.15343. This varied from that of aignopsanoic acid A (**6**)<sup>35</sup> by addition of  $H_2O$ . These two compounds exhibited parallel  $^1H$  and  $^{13}C$  NMR data (see Table S1) with the single distinction that the vinyl resonances were replaced by the two methine signals at  $\delta_H$  3.20 and  $\delta_H$  3.86, plus that of an OH ( $\delta_H$  8.6). The C-11 ( $\delta_C$  72.4)  $sp^3$  carbon was deduced to be a secondary alcohol from DEPT data and key 2D NMR data in Figure 3 showing diagnostic<sup>2-3</sup>  $J_{H,C}$  HMBC correlations observed from H-11 to the carbonyl carbons C-9 ( $\delta_C$  215.9) and C-12 ( $\delta_C$  178.8). Additional evidence for the *cis* decalin chair-chair orientation was derived from the 1-2 trans diaxial couplings ( $J = 14.4$  Hz) observed from H-6<sub>ax</sub> to H-7<sub>ax</sub>. NOESY data in Figure 3 showed that all three methyl groups plus H-8 were on the same side of a plane. This was consistent with reports for **6**, where the absolute configuration at positions C-4, C-5, C-10 was confirmed using CD measurements.<sup>35</sup> Based on a biosynthetic analogy to **6**, we have named this new compound aignopsanoic acid B (**13**) and conditionally assign its four stereocenters as 4*S*, 5*R*, 8*S*, 10*S* with position 11 remaining undefined. It is reasonable to conclude that **13** could serve as an important biogenetic precursor to **6** and vice versa.

Analysis of the compound listed as entry 6 (Fraction H33, 404  $m/z$ ) began by noting it displayed diagnostic  $\delta_H$ ,  $\delta_C$  values (see Table S2) similar to latrunculin A (**10**).<sup>27</sup> However key resonances of the hemiacetal and thiazolidinone moieties were altered. A molecular formula of  $C_{22}H_{31}NO_5SNa$  was set from HRESITOFMS data based on the  $[M + Na]^+$  ion  $m/z$  444.1782, which indicated eight degrees of unsaturation. These matching empirical data suggested a constitutional isomer of **10**. The  $^1H$  and  $^{13}C$  NMR shifts indicated a polyketide pattern from C-1 to C-10 as in **10** but with a terminal carboxylic acid group and modified thiazolidinone side chain suggesting an acyclic derivative. This was confirmed by significant  $^1H$ - $^1H$  COSY data of H-4 to H-11 and<sup>2-3</sup>  $J$ -HMBC correlations of H-2, H<sub>3</sub>-21 and H<sub>3</sub>-22 shown in Figure 3. Evidence of the free acid was supported by the existence of a broad singlet ( $\delta_H$  10.2) and acid carbonyl at C-1 ( $\delta_C$  169.6). Key differences observed for the remaining atoms C-11 to C-20 involved: a) the replacement of a methine by a methylene at C-15 ( $\delta_C$  19.9), suggesting the opened macrolide ring and b) the substitution of a hemiacetal carbon with an  $\alpha,\beta$ -unsaturated carbonyl at C-17 ( $\delta_C$  188.7) adjacent to  $sp^2$  carbons C-18 ( $\delta_C$  134.2) and C-19 ( $\delta_C$  114.8). These new functionalities, along with the presence of a carbonyl C-20 ( $\delta_C$  171.7) accounted for all eight degrees of unsaturation. Placement of the  $sp^2$  carbons was confined to the 4-thiazolin-2-one ring as evident from<sup>2-3</sup>  $J$ -HMBC correlations of H-19 ( $\delta_H$  7.10) to C-17, C-18 and C-20. Additional COSY data of H-15 ( $\delta_H$  1.74, 1.81) to H-16 ( $\delta_H$  2.73, 2.74) along with<sup>2-3</sup>  $J$ -HMBC correlations from H-11 to C-13 ( $\delta_C$  71.3); H-13 ( $\delta_H$  3.61) to C-15, and H-15, H-16 to C-17 secured the working structure presented in Figure 3. Overall this structure bears resemblance to the acyclic latrunculin B derivative latrunculin T<sup>43</sup> therefore we have named this latrunculin A (**10**) derivative apo latrunculin T (**14**). Latrunculin T has shown superior antifungal activity against *Saccharomyces cerevisiae* compared to either of the macrolides latrunculin A or B.<sup>40</sup> Interestingly **14** displayed activity in Table 1 against the parasite *T. brucei* but did not disrupt MF assembly at 20  $\mu g/mL$  suggesting a mode of action independent of the actin pathway similar to reports by others.<sup>27, 42</sup>

The geometries at  $\Delta^{2,3}$  and  $\Delta^{8,9}$  of **14** were designated *Z* based on the  $^{13}C$  chemical shift value for  $CH_3$ -21 ( $\delta_C$  24.5) and observed  $J$  values for H-8 and H-9 (10.8 Hz) while position  $\Delta^{6,7}$  was assigned as *E* from  $J$ -based analysis of H-6 and H-7 (15.0 Hz). These values were in accordance of those reported for **10**.<sup>27</sup> The orientation of the remaining asymmetric centers was provisionally assigned as 10*S*, 13*S* from NOESY data in Figure 3 showing correlations of H-10 ( $\delta_H$  2.61) to H-13 suggesting both protons were in the  $\beta$  position. Also from a biosynthetic perspective, all previously reported natural latrunculins retain these

configurations (or the equivalent as a function of differing numbering schemes).<sup>27, 43</sup> Compound **14** could serve as a putative biogenetic precursor to **10** in a similar manner previously described for the production of latrunculin B from latrunculin T.<sup>43</sup>

The analysis of entry 14 (Fraction H57, 513 *m/z*) NMR data (see Table S3) showed it was a fijianolide A (**9**)<sup>28</sup> derivative with an OCH<sub>3</sub> ( $\delta_{\text{H}}$  3.15,  $\delta_{\text{C}}$  49.2) present. This was supported by the molecular formula of C<sub>31</sub>H<sub>44</sub>NO<sub>8</sub> derived from HRESITOFMS data based on the [M+Na]<sup>+</sup> ion *m/z* ion of 567.29184 indicating an extra carbon, oxygen and two hydrogens. Major NMR shift differences observed for H-17 ( $\delta_{\text{H}}$  5.65), H-19 ( $\delta_{\text{H}}$  4.61) and C-20 ( $\delta_{\text{C}}$  109.0) compared with those of **9**,<sup>28</sup> suggested the OCH<sub>3</sub> was near the furan ring. This was supported by 2D NMR in Figure 3 which showed a key<sup>2</sup> *J* HMBC correlation from the OCH<sub>3</sub> to C-20 followed by<sup>2-3</sup> *J* -HMBC correlations from H-18 ( $\delta_{\text{H}}$  2.60, 2.03), H-19 to C-20 and H-21 ( $\delta_{\text{H}}$  5.84) to C-20, C-22 ( $\delta_{\text{C}}$  137.5) along with <sup>1</sup>H-<sup>1</sup>H COSY data of H-18 to H-19 and H-22 ( $\delta_{\text{H}}$  6.35) to H-23 ( $\delta_{\text{H}}$  3.90). The <sup>13</sup>C  $\delta$  values of the remaining atoms were  $\leq$  1.0 ppm of those of **9**, except for C-2, C-3 and C-13, which were verified with<sup>2-3</sup> *J* -HMBC correlations. These data secured the overall working structure as 20-methoxy-fijianolide A(**15**). The configurations at positions  $\Delta^{2,3}$ ,  $\Delta^{6,7}$  and  $\Delta^{25,26}$  were assigned as *Z* based on the identical ( $\leq$  1.0 ppm) <sup>13</sup>C values reported for **9**.<sup>28</sup> The configurations of six of the nine stereogenic centers were designated as 5*R*, 9*R*, 11*S*, 15*S*, 16*S*, 23*S* based also on matching <sup>13</sup>C  $\delta$  values. The remaining three positions were provisionally assigned 17*R*, 19*S*, 20*R* from NOESY data in Figure 3 that showed correlations from the OCH<sub>3</sub> to H-16 ( $\delta_{\text{H}}$  4.01) and H-17 ( $\delta_{\text{H}}$  5.65) indicating both sets were orientated on the same side of the plane. Modest MT stabilizing effects were seen for **15** in Table 1 confirming this assay can rapidly identify new compounds with MT cytoskeletal activity.

The final new compound, entry 16 (Fraction H61, 249 *m/z*) possessed a molecular formula of C<sub>17</sub>H<sub>28</sub>O<sub>3</sub> determined from the HRESITOFMS data based on the [M+Na]<sup>+</sup> *m/z* ion of 303.1918. This represented the loss of one degree of unsaturation versus that of **6**. The <sup>1</sup>H and <sup>13</sup>C NMR data (see Table S4) indicated a substitution of the exocyclic double and acid moiety for a di-methoxy ethyl side chain with OCH<sub>3</sub> groups ( $\delta_{\text{H}}$  3.33,  $\delta_{\text{C}}$  53.5, 53.7), methylenes C-11 ( $\delta_{\text{H}}$  2.54, 2.46;  $\delta_{\text{C}}$  34.1), and a methine C-12 ( $\delta_{\text{H}}$  4.51,  $\delta_{\text{C}}$  103.4). A rearranged  $\alpha$ ,  $\beta$ -unsaturated ketone C-9 ( $\delta_{\text{C}}$  204.1) with an endocyclic double C-8 ( $\delta_{\text{C}}$  133.1), C-7 ( $\delta_{\text{H}}$  6.53,  $\delta_{\text{C}}$  142.7) was also apparent. These conclusions accounted for the loss of one degree of unsaturation and were supported by 2D NMR data in Figure 3 showing<sup>2</sup> *J* HMBC correlations from the OCH<sub>3</sub> groups to C-12, <sup>1</sup>H - <sup>1</sup>H COSY data from H-12 to H-11 and<sup>2-3</sup> *J* -HMBC correlations from H-11 to C-7 - C-9. Additional COSY data from H-7 to H-6 ( $\delta_{\text{H}}$  2.39, 2.29) followed by<sup>2-3</sup> *J* -HMBC correlations from H-7 to C-9; H-6 to C-5 ( $\delta_{\text{C}}$  41.4), C-10 ( $\delta_{\text{C}}$  50.7) and H<sub>3</sub>-15 ( $\delta_{\text{H}}$  0.98) to C-9, C-10 linked the B ring together in only one way as aignopsane ketal (**16**). The remaining atoms (C-1 to C- 5 and C-13 to C-15) displayed <sup>13</sup>C NMR with values  $\leq$  1 ppm of those of **6**, confirming the existence of the A ring and the overall working structure of **16**. The geometry of  $\Delta^{7,8}$  was assigned as *Z* based on the observed vicinal coupling of 6.0 Hz between H-6 and H-7 that was in agreement with blancasterol<sup>47</sup> which shares a similar  $\alpha$ , $\beta$ -unsaturated ketone motif. Determination of the relative configuration of the asymmetric centers was set from NOESY data in Figure 3 which paralleled **13**, indicating the 4*S*, 5*R*, 10*S* orientation. It's possible to conclude that the unique structure of **16** arose from either **6** or **13** after a 48h exposure to MeOH-H<sub>2</sub>O during processing and or transport, which may have lead to the formation of it's dimethyl acetal functionality.

Although the above exemplar served to rapidly identify distinct bioactive natural products and several new compounds, one particular issue involving its application deserves discussion. Further efforts screening extracts of additional sponges and microorganisms led to several false positives with selected examples involving the compounds displayed in

Figure 4. These compounds were identified as active library fractions based on inaccurate fraction weight concentrations used when assaying library wells. Typically natural product HPLC well plate library fractions are assayed based on averaging the amount injected on the column divided by the number of library fractions wells to arrive at an assumed amount per well.<sup>13–15</sup> This approach proved practical when assaying complex extracts such as in Figure 1. However when assaying extracts consisting of only 1–2 major metabolites contained in only a few library fraction wells, with the remaining library fraction wells being devoid of compounds, these libraries plates must be viewed with caution. Our results indicated these library fractions could appear an order of magnitude more potent versus data obtained from re-assay using accurate weights.

A further illustration of misleading analyses of libraries containing just a few major compounds culminating in the conclusion of false positives involves the situation depicted in Figure 5. The hexanes extract (sample coded FH) of a sponge (*Spongia* species, coll. no. 92503) appeared to have several metabolites with varying concentrations using ELSD and UV (230nm) detection. Although LC-MS analysis with ELSD is often regarded as a reliable indicator of actual sample concentrations, detector response factors can be affected by the nature of the solvent and analytes.<sup>10</sup> As an example the <sup>1</sup>H NMR spectrum (see Figure S45) of this extract indicated the presence of just one major metabolite that was later confirmed as the active component in the LC-MS-UV-ELSD library fraction 92503 FH H27 in Figure 5a when tested at 10 µg/mL with an assumed weight of 0.1 mg. This library fraction displayed cytotoxicity on par with the standard doxorubicin<sup>48</sup> at 10 µM against macrophage (RAW 264.7) cells. After scale up isolation / de-replication the structure proved to be the common sponge diterpene, spongia- 13(16),-14-dien-19-oic acid (**17**).<sup>49</sup> Unfortunately when re-assayed as a pure compound with a measured weight (in mgs) it required a concentration ≥ 90 µM to achieve the same cytotoxicity seen previously alongside doxorubicin at 10 µM.

We now believe one way to avoid the bioassay variability described above is to use removable 96 well library plates, which can provide actual measured weights per well for the assay activity calculation. An example of this approach is outlined in Figure 5b. Reevaluation of the extract coll. no. 92503 FH indicated the library fraction 92503 FH H27 accounted for approximately ≥ 4.0 mg of the 10.0 mg extract and when the fraction was assayed using this amount (at 10 µg/mL) it was significantly less cytotoxic than doxorubicin at 10 µM. In terms of the bioassay data seen here, this sample would not constitute a priority lead to undergo automated scale up HPLC. Similar results were encountered with bioactive microbial extracts provided by the Phaff yeast collection<sup>50</sup> UC Davis as well as from Indonesian fungal samples. Selected examples include coll. nos. UCDFST 05565 L, and LIPI 010A5 L (see Figures S46, S48). Using the standard library approach these samples displayed cytotoxicity against prostate (PC3) cancer cell lines equal to or greater than doxorubicin at 10 µM. Upon reexamination using removable well libraries, we concluded that the initially active library fractions from samples 05565 L H10 and 010A5 L H29 which contained penicillic acid (**18**)<sup>51</sup> and hexylcinnamaldehyde (**19**)<sup>52</sup> (Figure 4) were false positives as they displayed markedly diminished cytotoxicity.

We now recommend examining <sup>1</sup>H NMR data alongside the LC-MS-ELSD trace of a bioactive crude extract sample under analysis. This approach provides clarity on the issue of the metabolite complexity and assists in the decision on whether to generate a standard or a removable well library. A clear advantage of this can be seen when comparing the <sup>1</sup>H NMR spectra of a complex versus simple extracts such as in coll. no. 07327 F XFD (see Figure S5) versus coll. nos. 92503 FH, 05565 L and 010A5 L (see Figures S45, S47, S49). While the former extract indicates a multitude of metabolites, the latter extracts are clearly enriched with only one or two. Applying removable well LC-MS-UV-ELSD libraries to the latter cases is essential to avoid outcomes involving HT bioassay false positives.

## Conclusions

There are a number of lessons learned from the HT survey of marine sponge and microbial extracts involving the outline shown in Scheme 1. A key element of this strategy involves the creation and evaluation of LC-MS-UV-ELSD libraries. First, we have shown that once a bioactive extract is identified, preparation of reduced complexity library fractions prior to bioassays can pinpoint lead compounds in just one step, eliminating multiple rounds of time consuming bioassay guided fractionation. Second, a multi-assayed approach can be useful to identify new or known natural products with previously unreported biological activities as illustrated by the cases of the lead compounds **1** and **11**. Third, applications of ELSD are advantageous for detecting known or new compounds devoid of a UV-chromophore (e.g., **12**, **13**) however it is not always a reliable method for determining concentrations of disparate metabolites in an extract. Lastly, use of removable well libraries to screen extracts containing only 1–2 major metabolites can reduce the incidents of false positives that occur during bioassay evaluations of HPLC-based natural product libraries.

We have now used the HT methods of Scheme 1 to screen several hundred extracts from marine sponges, plants and microbial sources as part of our ICBG collaborations and these investigations will be reported in due course. Our findings in this study illustrate that using automated LC-MS-UV-ELSD libraries that are compatible with current HTS bioassays significantly reduces the cycle times required to discover bioactive lead compounds and or new molecular structures. These results and those recently published by others<sup>9–17</sup> demonstrate the power of applying modern HT methods in natural products-based research to streamline therapeutic lead discovery programs.

## Experimental Section

### General Experimental Procedures

Crude extractions were obtained using an accelerated solvent extractor (ASE) or with traditional methods reported previously.<sup>18, 19</sup> Optical rotations were obtained on a JASCO DIP-370 digital polarimeter while  $UV_{max}$  data was obtained using a Waters 996 PDA detector. All NMR experiments were run on a Varian UNITY 500 (500 and 125 MHz for  $^1H$  and  $^{13}C$ , respectively) or Varian INOVA 600 spectrometer (600 and 150 MHz for  $^1H$  and  $^{13}C$  respectively). The 600 MHz spectrometer was equipped with a 5mm triple resonance (HCN) cryogenic probe. Sample amounts smaller than 2.0 mg were analyzed using 3 and 5 mm Shigemi tubes where available. High resolution mass spectrometry measurements were obtained using a Mariner ESI-TOF-MS. Analytical LC-MS analysis was performed on samples at a concentration of approximately 5 mg/mL, using a reversed-phase  $150 \times 4.60$  mm  $5 \mu m$  C<sub>18</sub> Phenomenex Luna column in conjunction with a  $4.0 \times 3.0$  mm C18 (Octadecyl) guard column and cartridge (Holder part number: KJ0-4282, Cartridge part number: AJ0-4287, (Phenomenex, Inc., Torrance, CA). Samples were injected onto the column using a volume of 15  $\mu L$ , with a flow rate of 1 mL/min that was monitored using a Waters model 996 photodiode array (PDA) UV detector. The elution was subsequently split (1:1) between a S.E.D.E.R.E. model 55 evaporative light scattering detector (ELSD), and an Applied Biosystems Mariner electrospray ionization time of flight (ESI-TOF) mass spectrometer.

### Biological Material, Collection and Identification

Specimens of the sponge *Cacospongia mycofijiensis* profiled for these experiments (coll. nos. 07327 **A–J**, **L–O**, 387 g wet wt.) were collected in 2007 off the northern coastlines of New Britain, Papua New Guinea.<sup>35</sup> Taxonomic identifications were based on comparison of the biological features to other voucher samples in our repository and confirmed by Nicole J.



de Voogd of the National Museum of Natural History, the Netherlands. The secondary metabolite chemistry is also consistent with these identifications. Voucher specimens and underwater photos are available. The extract of sample coll. no. 92503 was identified as belonging to the genus *Spongia* and was obtained from the UCSC marine natural products repository as an archived 1992 Indonesian expedition sample. Taxonomic identification was performed by Christina Diaz. The filamentous fungus UCDFST 05565 was provided by the Phaff Yeast Culture Collection<sup>50</sup> UC Davis and identified as *Hyalodendriella betulae* while the microbial sample coll. no. 010A5 was an unidentified filamentous fungus specimen provided by the Research Center for Biology & Chemistry, Indonesian Institute of Science (LIPI).

### Extraction and Prefractionation

Sponge samples were preserved in the field by being immersed in a 50-50 MeOH:H<sub>2</sub>O solution. After approximately 48 h this solution was decanted and discarded. The damp organisms were placed in collection bottles (Nalgene) and shipped back to UCSC at ambient temperature and then stored at 4 °C until further processed. Specimens of *C. mycofijiensis* coll. nos. 07327A–J, L–O (387 g wet wt.) were processed using the high-throughput method of accelerated solvent extraction (ASE)<sup>19</sup> to generate four extracts sequentially. Samples were first extracted with H<sub>2</sub>O, to remove inorganic salts (sample coded XWW), followed by hexanes to remove unwanted steroid and lipid components (sample coded XFH), CH<sub>2</sub>Cl<sub>2</sub> (sample coded XFD) and MeOH (sample coded XFM). Samples 07327 F afforded: 221.2 mg, XWW; 42.3 mg, XFH; 78.2 mg, XFD and 56.5 mg, XFM extracts. The repository *Spongia* specimen (coll. no. 92503) was extracted using traditional methods of solvent partitioning.<sup>19</sup> Plant materials were extracted with MeOH and hexanes. Methanol extracts of these samples were further fractionated with solid phase extraction (SPE) cartridges to remove polyphenols using a 700 mg polyamide-filled cartridge (Sigma-Aldrich, St. Louis, MO) according to reported methods.<sup>12</sup> Microbial specimens coll. nos. 05565 (*H. betulae*) and 010A5 were extracted using traditional methods involving EtOAc and MeOH.<sup>18</sup>

### LC-MS-UV-ELSD with Fraction Collection and Scale Up Isolation

A representation of the LC-MS-UV-ELSD instrumentation setup is shown in Figure S50. LC-MS-UV-ELSD analysis was performed using two Waters 510 pumps, controlled with Empower 2 software. A Waters 717plus autosampler was used for sample loading and injection. Separation was performed on a Luna 5 µm, C18(2) 100Å 10 × 250 mm column (Phenomenex, Inc.) in conjunction with a guard column using a larger 10.0 × 10.0 mm C18 (ODS) cartridge (Holder part number: AJ0-7220, Cartridge part number: AJ0-7221). Spectra from three detectors were acquired during each run; Waters 996 photo diode array, SEDEX 55 ELSD and Mariner 5054 ESI-TOF-MS. Solvent flow was controlled through backpressure regulation. A simple low dead volume cross union from IDEX Health & Science was used to split solvent. Desired flow rates were used to determine the appropriate tubing diameter and length. A solvent flow rate of 1.9 mL/min of solvent flowing, to the fraction collector, through 60 inches of 0.01” inner diameter (ID) tubing will result in 68.5 psi of back pressure. Solvent flowing at a rate of 0.08 mL/min, to the ELSD through 36 inches of .004” ID tubing, will result in 67.6 psi of back pressure. Solvent flowing at a rate of 0.02 mL/min to the mass spectrometer through 22 inches of .0025” ID tubing results in 67.7 psi of backpressure. All values of psi were calculated using a viscosity of 1. Some time delay between instrumentation will happen, but has been kept to a minimum. The mobile phase parameters are CH<sub>3</sub>CN (A) and H<sub>2</sub>O (B) with a flow rate of 2 mL/min and a gradient of: 0 min, 10:90; 40 min 100:0; 60 min, 100:0. Injection amounts range from [10 mg/100–150 µL] to [15 mg/150–200 µL].

Sample collection was performed using a Gilson 215 liquid handler controlled with Gilson Unipoint LC software. Samples were collected into BD Biosciences 96 deep-well plates, with a working volume of 2 mL (Part number: 353966). Simport Plastics 96 removable-well plates (Part number: T105-50) were also used, and allowed each sample well to be pre-weighed and reweighed after sample collection for accurate sample weight determination. Scale up HPLC fractions were collected into 20 mL scintillation vials using two Gilson collection racks (number coded 204). Alternatively larger HPLC scale up fractions can be generated using 50 mL test tubes with the 2 Gilson collection racks (number coded 225). Fractions were collected every minute. Sample workup sheets for standard and removable 96 well plates are shown in Figures S51–S52. An example of proper weighing technique using removable 96 well plate libraries to maximize accuracy is shown in Figure S53.

After the LC-MS-UV-ELSD library is collected, a duplicate plate is generated for analytical reference using a 12-channel pipette, creating an exact copy and counter balance for centrifugal drying. Plates were dried and concentrated using a Savant AES2010 SpeedVac. Dried plates were reconstituted in DMSO to a concentration of either 10 or 20  $\mu\text{g/mL}$  for bioassay unless otherwise specified.

The XFD extract (78.2 mg) of coll. no 07327 F was used to prepare four LC-MS-UV-ELSD libraries into 96 well plates (40.1 mg,  $[10\text{mg}/100\ \mu\text{L}] \times 4$  injections) for eight HT bioassay evaluations using a modified gradient of 30:70 to 80:20  $\text{CH}_3\text{CN}:\text{H}_2\text{O}$  over 70 minutes to maximize baseline peak separation. Reference libraries were generated from each of the four original libraries using a 12-channel pipette, creating an exact copy and counter balance for centrifugal drying. Using the remaining 38.1 mg, automated scale up HPLC into 20 mL vials ( $[9.5\text{mg}/100\ \mu\text{L}] \times 4$  injections) was performed with the same 5  $\mu\text{m}$  column and conditions used for the LC-MS-UV-ELSD library purifications. Reference library well fractions were combined with corresponding 20 mL HPLC vial fractions based on parallel LC-MS-UV-ELSD data to provide the total amounts of the selected pure compounds as: H20 latrunculol A (**1**, 4.6 mg), H22 latrunculone A (**2**, 1.2 mg), H28 latrunculol B (**3**, 1.3 mg), H37 latrunculone B (**4**, 2.1 mg), H38 fijianolide D (**5**, 2.1 mg), H44 aignopsanoic acid A (**6**, 4.8 mg), H59 methyl aignopsanoate (**7**, 1.5 mg), H47 fijianolide B (**8**, 2.7 mg), H52 fijianolide A (**9**, 2.3 mg), H54 latrunculin A (**10**, 4.6 mg), H56 mycothiazole (**11**, 1.9 mg), H65 sacrotride A (**12**, 1.3 mg), H30 aignopsanoic acid B (**13**, 1.4 mg), H33 apo-latrunculin T (**14**, 1.7 mg), H57 20-methoxy-fijianolide A (**15**, 1.0 mg), and H61 aignopsane ketal (**16**, 1.3 mg).

The hexanes extract (sample coded FH, 1.2 g) of the sponge sample *Spongia* coll. no. 92503 was used to make an LC-MS-UV-ELSD standard library involving a 10 mg/100  $\mu\text{L}$  injection using a gradient of 10:90 to 100:0  $\text{CH}_3\text{CN}:\text{H}_2\text{O}$  over 50 min. The library was transferred into a duplicate well plate for reference using a 12-channel pipette, creating an exact copy and counter balance for centrifugal drying. A second removable well library was also generated using the same conditions and above protocol. The amounts of the pre and post tared weights per well were measured using a Mettler AE 200 analytical balance. An example of the removable well library weighing protocol is outlined in Figure S53. Reference fractions of both standard and removable well libraries were combined (based on parallel LC-MS-UV-ELSD data) with one automated scale up HPLC injection  $[10.0\ \text{mg}/100\ \mu\text{L}]$  that was fractionated into a 20 mL vial (fraction H27) to yield pure spongia-13(16),-14-dien-19-oic acid (**17**, 5.3 mg).

The EtoAc extract (sample coded L, 16.4 mg) of the yeast specimen *H. betulae* coll. no. 05565 was used to make an LC-MS-UV-ELSD standard library involving a 10 mg/100  $\mu\text{L}$  injection using a gradient of 10:90 to 100:0  $\text{CH}_3\text{CN}:\text{H}_2\text{O}$  over 50 minutes. The library was transferred into a duplicate well plate for reference using a 12-channel pipette, to create an exact copy and counter balance for centrifugal drying. A second removable well library was

also generated using the same conditions and above protocol. The amounts of the pre and post tared weights per well were measured using a Mettler AE 200 analytical balance. Reference fractions of both standard and removable well libraries were combined (based on parallel LC-MS-UV-ELSD data) with one automated scale up HPLC injection [6.0 mg/100  $\mu$ L] that was fractionated into a 20 mL vial (fraction H10) to yield pure penicillic acid (2.3 mg).<sup>51</sup>

The EtoAc extract (sample coded L, 39.5 mg) of the unidentified filamentous fungi specimen coll. no. 010A5 was used to make an LC-MS-UV-ELSD standard library involving a 10 mg/100  $\mu$ L injection using a gradient of 10:90 to 100:0 CH<sub>3</sub>CN: H<sub>2</sub>O over 50 min. The library was transferred into a duplicate well plate for reference using a 12-channel pipette, to create an exact copy and counter balance for centrifugal drying. A second removable well library was also generated using the same conditions and above protocol. The amounts of the pre and post tared weights per well were measured using a Mettler AE 200 analytical balance. Reference fractions of both standard and removable well libraries were combined (based on parallel LC-MS-UV-ELSD data) with one automated scale up HPLC injection [10.0 mg/100  $\mu$ L] that was fractionated into a 20 mL vial (fraction H29) to yield pure hexyl cinnamaldehyde (4.2 mg).<sup>52</sup>

### Cytoskeletal Assay

HeLa cells were plated in 384-well tissue culture treated plates (Corning 3712) at a density of 1500 cells per well. After incubating at 37 °C with 5% CO<sub>2</sub> overnight extracts and library well fractions were pinned into plates using the Janus MDT (PerkinElmer). After 24 h cells were fixed in 4% formaldehyde for 20 min, then washed with PBS using an automated plate washer (BioTek). The cells were then treated with 0.5% TritonX-100 in PBS for 10 min, washed, and then blocked with a 2% BSA PBS solution for 20 min. Actin was stained with rhodamine-phalloidin (synthesized according to reported methods<sup>53</sup>) for 20 min and then washed. Lastly, the DNA was stained with Hoechst 33342 (AnaSpec Inc.) followed by a wash with the automated plate washer. The plates are then stored in a 0.1% azide PBS solution. Images were taken using the ImageXpress (Molecular Devices) automated fluorescence microscope at a 10 $\times$  magnification.

### *Trypanosoma brucei brucei* Assay

The growth inhibition assay for *T. brucei brucei* was conducted as described previously.<sup>22</sup> Bloodstream forms of the monomorphic *T. b. brucei* clone 427-221a were grown in complete HMI-9 medium containing 10% FBS, 10% Serum Plus medium (Sigma Inc.), 50 U/mL penicillin and 50  $\mu$ g/mL streptomycin (Invitrogen) at 37° C under a humidified atmosphere and 5% CO<sub>2</sub>. Extracts and library well fractions were screened at 12.5  $\mu$ g/mL and 1.25  $\mu$ g/mL for % inhibition values or serially diluted in the range of 25  $\mu$ g/mL – 0.001  $\mu$ g/mL for IC<sub>50</sub> determinations. 0.5  $\mu$ L of each dilution was added to 100  $\mu$ L of diluted parasites (1 $\times$ 10<sup>4</sup> cells per well) in sterile Greiner 96-well flat white opaque culture plates such that the final DMSO concentration was 0.5%. 0% Inhibition control wells contained 0.5% DMSO while 100% inhibition control wells contained 50  $\mu$ M thimerosal (Sigma). After compound addition, plates were incubated for 40 hours at 37 °C. At the end of the incubation period, 50  $\mu$ L of CellTiter-Glo reagent (Promega Inc.) was added to each well and plates were placed on an orbital shaker at room temperature for 2 min to induce lysis. After a 10 min incubation to stabilize the signal, the ATP-bioluminescence of each well was determined using an Analyst HT plate reader (Molecular Devices). Raw values were converted to log<sub>10</sub> and percentage inhibition calculated relative to the controls. IC<sub>50</sub> curve fittings were performed with Prism 4 software as above.

## Antiproliferative Bioassays

Antiproliferative effects of extracts and library well fractions were evaluated in four cultured human cancer cell lines shown in Table 1. The cells were placed into 96-well plates and grown in the absence or continuous presence of 1.5–50 000 nM test compounds for 96 h as reported previously.<sup>23</sup> Cell growth was assessed using the CellTiter-Glo luminescent cell viability assay (Promega) according to the manufacturer's recommendations. Luminescence was read on a Victor2V 1420 MultiLabel HTS counter (Perkin-Elmer/Wallac). IC<sub>50</sub> values were determined as the concentration of a compound that inhibits cell growth by 50% compared to untreated cell populations. Two separate replicate experiments were performed.

**MTT Cytotoxicity Assay**—Extracts and library well fractions were tested at 10 and 20 µg/mL respectively using a previously reported MTT assay<sup>18</sup> in murine macrophage (RAW264.7) and prostate cancer (PC3) cell lines to determine cytotoxic activity. Cells in 96-well plates in the required growth medium were treated with extracts dissolved in DMSO for 20 h (RAW264.7). After incubation, MTT solution was added to the wells and incubated for another 2 h. Media were removed and DMSO was added to dissolve purple precipitates. Then plates were read at 570 nm using a plate reader.

Compounds **1–12** and **17–19**: The known compounds were identified by comparison of spectroscopic data with those of literature values (See Supporting Information for <sup>1</sup>H NMR and LRMS data, as well as literature references).

**Aignopsanoic acid B (13)**: white amorphous powder; [ $\alpha$ ]<sup>23</sup><sub>D</sub> -6.0 (*c* 0.05, MeOH); <sup>1</sup>H and <sup>13</sup>C NMR data in Table S1 in Supporting Information. LRESITOFMS *m/z* 291.1 [M + Na]<sup>+</sup>, 269.1 [M + H]<sup>+</sup>, HRESITOFMS *m/z* 291.1547 [M + Na]<sup>+</sup> (calcd for C<sub>15</sub>H<sub>24</sub>O<sub>4</sub>Na, 291.1556).

**Apo-latrunculin T (14)**: white oil; [ $\alpha$ ]<sup>23</sup><sub>D</sub> +41 (*c* 0.1, MeOH); UV (CH<sub>3</sub>CN/H<sub>2</sub>O/0.1% formic acid)  $\lambda$ <sub>max</sub> 236, 290 nm; <sup>1</sup>H and <sup>13</sup>C NMR (see Table S2 In Supporting Information); HRESIMS *m/z* 444.1782 [M + Na]<sup>+</sup> (calcd for C<sub>22</sub>H<sub>31</sub>NO<sub>5</sub>Na, 444.1815).

**20-methoxy-fijianolide A (15)**: white oil; [ $\alpha$ ]<sup>23</sup><sub>D</sub> -67 (*c* 0.1, MeOH); UV (CH<sub>3</sub>CN/H<sub>2</sub>O/0.1% formic acid)  $\lambda$ <sub>max</sub> 224 nm; <sup>1</sup>H and <sup>13</sup>C NMR (see Table S3); LRESITOFMS *m/z* 513.1. [M - CH<sub>3</sub>OH + H]<sup>+</sup>, HRESIMS *m/z* 567.29184 [M + Na]<sup>+</sup> (calcd for C<sub>31</sub>H<sub>44</sub>NO<sub>8</sub>Na 567.29284).

**Aignopsane ketal (16)**: white amorphous oil. [ $\alpha$ ]<sup>23</sup><sub>D</sub> 32 (*c* 0.05, MeOH); UV (CH<sub>3</sub>CN/H<sub>2</sub>O/0.1% formic acid)  $\lambda$ <sub>max</sub> 217 nm; <sup>1</sup>H and <sup>13</sup>C NMR data in Table S4 in Supporting Information. LRESITOFMS *m/z* 249.1 [M - CH<sub>3</sub>OH + H]<sup>+</sup>, 303.1 [M + Na]<sup>+</sup>, HRESITOFMS *m/z* ion of 303.1918 [M + Na]<sup>+</sup> (calcd for C<sub>17</sub>H<sub>28</sub>O<sub>3</sub>Na, 303.1930).

## Supplementary Material

Refer to Web version on PubMed Central for supplementary material.

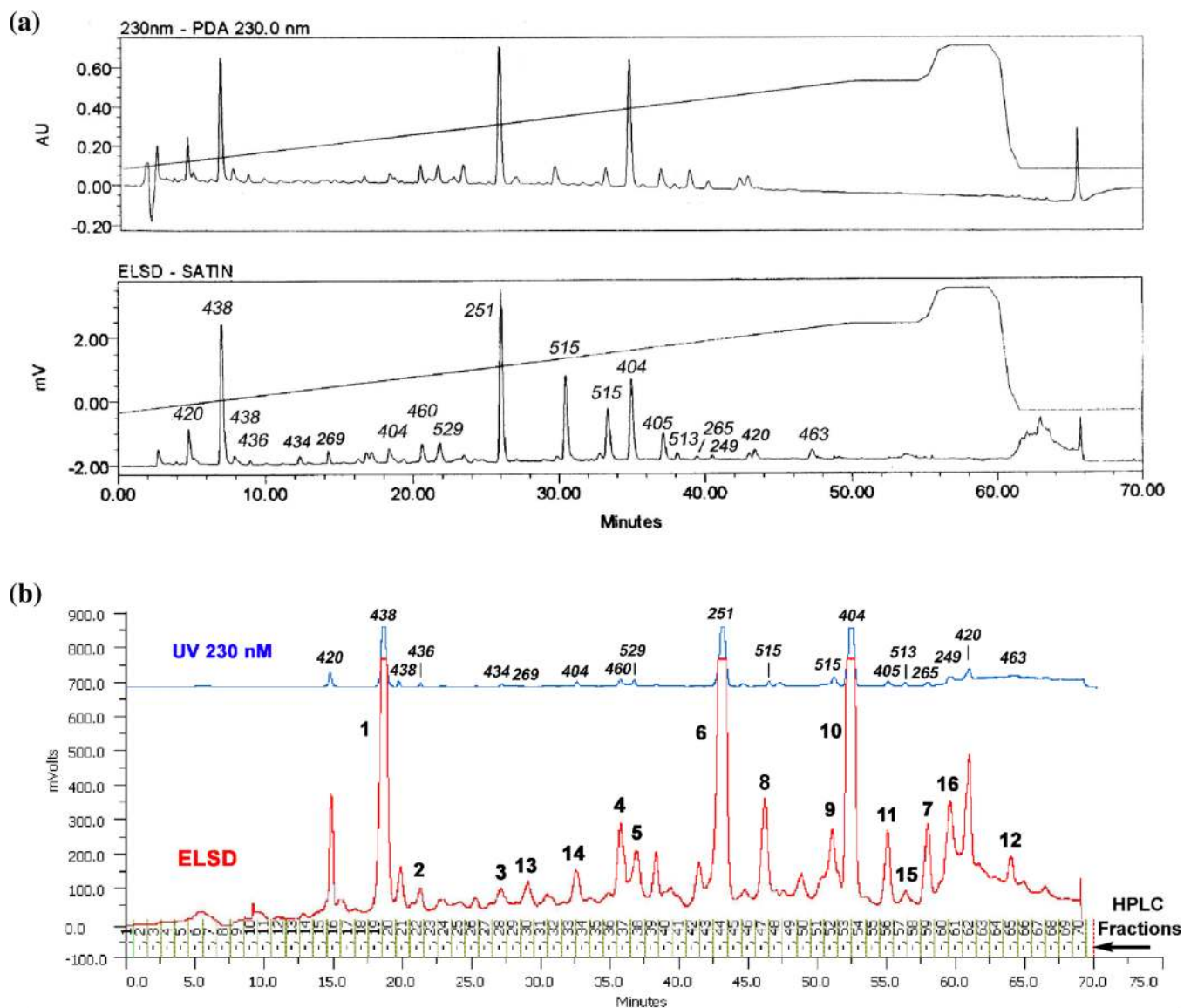
## Acknowledgments

This work was supported by grants from the NIH R01 CA 47135 (PC), and NIH Fogarty International Center, International Cooperative Biodiversity Groups. Award number 1U01TW008160-01 and Agricultural Food Research Initiative of the National Institute of Food and Agriculture, USDA, Grant #35621-04750 (LFB, KBM). Support also was obtained from the Sandler Family Foundation (PC), the California Institute for Quantitative Biosciences (PC, JM). We also grateful to Professor T. Matainaho (U PNG) for assistance in permit collection approval Papua New Guinea.

## References

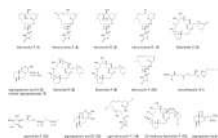
1. Li JWH, Vederas JC. *Science*. 2009; 325:161–165. [PubMed: 19589993]
2. Cragg GM, Grothaus PG, Newman DJ. *Chem. Rev.* 2009; 109:3012–3043. [PubMed: 19422222]
3. Rishton GM. *Am. J. Cardiol.* 2008; 101:43d–49d. [PubMed: 18243858]
4. Newman DJ, Cragg GM. *J. Nat. Prod.* 2007; 70:461–477. [PubMed: 17309302]
5. Koehn FE, Carter GT. *Nat. Rev. Drug. Discov.* 2005; 4:206–220. [PubMed: 15729362]
6. Kingston DGI. *J. Nat. Prod.* 2011; 74:496–511. [PubMed: 21138324]
7. [Accessed May 25, 2011] <http://www.fda.gov/Drugs/NewsEvents/UCM130961>
8. Danishefsky S. *Nat. Prod. Rep.* 2010; 27:1114–1116. [PubMed: 20383353]
9. Zeng L, Eldridge GR, Vervoort HC, Lee CM, Cremin PA, Williams CT, Hart SM, Goering MG, O'Neil-Johnson M. *Anal. Chem.* 2002; 74:3963–3971. [PubMed: 12199561]
10. Wolf D, Siems K. *Chimia.* 2007; 61:339–345.
11. Wagenaar MM. *Molecules.* 2008; 13:1406–1426. [PubMed: 18596666]
12. Tu Y, Jeffries C, Ruan H, Nelson C, Smithson D, Shelat AA, Brown KM, Li XC, Hester JP, Smillie T, Khan IA, Walker L, Guy K, Yan B. *J. Nat. Prod.* 2010; 73:751–754. [PubMed: 20232897]
13. Bugni TS, Richards B, Bhoite L, Cimbora D, Harper MK, Ireland CM. *J. Nat. Prod.* 2008; 71:1095–1098. [PubMed: 18505284]
14. Gassner NC, Tamble CM, Bock JE, Cotton N, White KN, Tenney K, St Onge RP, Proctor MJ, Giaeever G, Nislow C, Davis RW, Crews P, Holman TR, Lokey RS. *J. Nat. Prod.* 2007; 70:383–390. [PubMed: 17291044]
15. Lang G, Mitova MI, Ellis G, Van der Sar S, Phipps RK, Blunt JW, Cummings NJ, Cole ALJ, Munro MHG. *J. Nat. Prod.* 2006; 69:621–624. [PubMed: 16643039]
16. Mitova MI, Murphy AC, Lang G, Blunt JW, Cole ALJ, Ellis G, Munro MHG. *J. Nat. Prod.* 2008; 71:1600–1603. [PubMed: 18702471]
17. Lang G, Mayhudin NA, Mitova MI, Sun L, van der Sar S, Blunt JW, Cole ALJ, Ellis G, Laatsch H, Munro MHG. *J. Nat. Prod.* 2008; 71:1595–1599. [PubMed: 18710284]
18. Wu QX, Crews MS, Draskovic M, Sohn J, Johnson TA, Tenney K, Valeriote FA, Yao XJ, Bjeldanes LF, Crews P. *Org. Lett.* 2010; 12:4458–4461. [PubMed: 20866076]
19. Johnson TA, Morgan MVC, Aratow NA, Estee SA, Sashidhara KV, Loveridge ST, Segraves NL, Crews P. *J. Nat. Prod.* 2010; 73:359–364. [PubMed: 20030364]
20. Harvey AL, Cree IA. *Planta Med.* 2010; 76:1080–1086. [PubMed: 20635309]
21. Watts KR, Morinaka BI, Amagata T, Robinson SJ, Tenney K, Bray WM, Gassner NC, Lokey RS, Media J, Valeriote FA, Crews P. *J. Nat. Prod.* 2011; 74:341–351. [PubMed: 21241058]
22. Mackey ZB, Baca AM, Mallari JP, Apsel B, Shelat A, Hansell EJ, Chiang PK, Wolff B, Guy KR, Williams J, McKerrow JH. *Chem. Biol. Drug Des.* 2006; 67:355–363. [PubMed: 16784460]
23. Inman WD, Bray WM, Gassner NC, Lokey RS, Tenney K, Shen YYC, TenDyke K, Suh T, Crews P. *J. Nat. Prod.* 2010; 73:255–257. [PubMed: 20000782]
24. Nielsen CK, Simms JA, Pierson HB, Li R, Saini SK, Ananthan S, Bartlett SE. *Biol. Psychiatry.* 2008; 64:974–981. [PubMed: 18774553]
25. Buss, AD.; Butler, MS. Bugni, TS.; Harper, MK.; McCulloch, MWB.; Whitson, EL. *Natural Products Chemistry for Drug Discovery*. Cambridge, UK: RSC Publishing; 2010. p. 272-298.
26. Longley RE, McConnell OJ, Essich E, Harmody D. *J. Nat. Prod.* 1993; 56:915–920. [PubMed: 8350092]
27. Amagata T, Johnson TA, Cichewicz RH, Tenney K, Mooberry SL, Media J, Edelstein M, Valeriote FA, Crews P. *J. Med. Chem.* 2008; 51:7234–7242. [PubMed: 18942825]
28. Johnson TA, Tenney K, Cichewicz RH, Morinaka BI, White KN, Amagata T, Subramanian B, Media J, Mooberry SL, Valeriote FA, Crews P. *J. Med. Chem.* 2007; 50:3795–3803. [PubMed: 17622130]
29. Corley DG, Herb R, Moore RE, Scheuer PJ, Paul VJ. *J. Org. Chem.* 1988; 53:3644–3646.
30. Kakou Y, Crews P, Bakus GJ. *J. Nat. Prod.* 1987; 50:482–484.

31. Sonnenschein RN, Johnson TA, Tenney K, Valeriote FA, Crews P. *J. Nat. Prod.* 2006; 69:145–147. [PubMed: 16441088]
32. Morgan JB, Mahdi F, Liu Y, Coothankandaswamy V, Jekabsons MB, Johnson TA, Sashidhara KV, Crews P, Nagle DG, Zhou YD. *Bioorg. Med. Chem.* 2010; 18:5988–5994. [PubMed: 20637638]
33. Field JJ, Singh AJ, Kanakkanthara A, Halafihi T, Northcote PT, Miller JH. *J. Med. Chem.* 2009; 52:7328–7332. [PubMed: 19877653]
34. Johnson TA, Amagata T, Oliver AG, Tenney K, Valeriote FA, Crews P. *J. Org. Chem.* 2008; 73:7255–7259. [PubMed: 18715038]
35. Johnson TA, Amagata T, Sashidhara KV, Oliver AG, Tenney K, Matainaho T, Ang KKH, McKerrow JH, Crews P. *Org. Lett.* 2009; 11:1975–1978. [PubMed: 19385671]
36. Tanaka J, Higa T, Bernardinelli G, Jefford CW. *Chem. Lett.* 1996:255–256.
37. Watts KR, Tenney K, Crews P. *Curr. Opin. Biotechnol.* 2010; 21:808–818. [PubMed: 20956079]
38. Schirmeister T, Vicik R, Hoerr V, Glaser M, Schultheis M, Hansell E, McKerrow JH, Holzgrabe U, Caffrey CR, Ponte-Sucre A, Moll H, Stich A. *Bioorg. Med. Chem. Lett.* 2006; 16:2753–2757. [PubMed: 16516467]
39. Shaw J, Valeriote FA, Media J, Johnson TA, Amagata T, Tenney K, Crews P. *Anal. Bioanal. Chem.* 2010; 396:1741–1744. [PubMed: 20043220]
40. Kudrimoti S, Ahmed SA, Daga PR, Wahba AE, Khalifa SI, Doerksen RJ, Hamann MT. *Bioorg. Med. Chem.* 2009; 17:7517–7522. [PubMed: 19800245]
41. El Sayed KA, Khanfar MA, Shallal HM, Muralidharan A, Awate B, Youssef DTA, Liu Y, Zhou YD, Nagle DG, Shah G. *J. Nat. Prod.* 2008; 71:396–402. [PubMed: 18298079]
42. Ahmed SA, Odde S, Daga PR, Bowling JJ, Mesbah MK, Youssef DT, Khalifa SI, Doerksen RJ, Hamann MT. *Org. Lett.* 2007; 9:4773–4776. [PubMed: 17929935]
43. El Sayed KA, Youssef DT, Marchetti D. *J. Nat. Prod.* 2006; 69:219–223. [PubMed: 16499319]
44. Mahler G, Serra G, Dematteis S, Saldana J, Dominguez L, Manta E. *Bioorg. Med. Chem. Lett.* 2006; 16:1309–1311. [PubMed: 16384701]
45. Kim DK, Lim YJ, Kim JS, Park JH, Kim ND, Im KS, Hong J, Jung JH. *J. Nat. Prod.* 1999; 62:773–776. [PubMed: 10346968]
46. Costantino V, Fattorusso E, Imperatore C, Mangoni A. *J. Nat. Prod.* 2002; 65:883–886. [PubMed: 12088432]
47. Pika J, Andersen RJ. *Tetrahedron.* 1993; 49:8757–8760.
48. Hassan F, Islam S, Mu MM, Ito H, Koide N, Mori I, Yoshida T, Yokochi T. *Mol. Cancer Res.* 2005; 3:373–379. [PubMed: 16046548]
49. Capelle N, Braekman JC, Daloz D, Tursch B. *Bull. Soc. Chim. Belg.* 1980; 89:399–404.
50. Fell JW, Scorzett G, Statzell-Tallman A, Boundy-Mills K. *Fems. Yeast Res.* 2007; 7:1399–1408. [PubMed: 17825066]
51. He J, Wijeratne EMK, Bashyal BP, Zhan JX, Seliga CJ, Liu MPX, Pierson EE, Pierson LS, VanEttten HD, Gunatilaka AAL. *J. Nat. Prod.* 2004; 67:1985–1991. [PubMed: 15620238]
52. Talzi VP. *Russ. J. Appl. Chem.* 2006; 79:107–116.
53. Schuresko LA, Lokey RS. *Angew. Chem. Int. Edit.* 2007; 46:3547–3549.



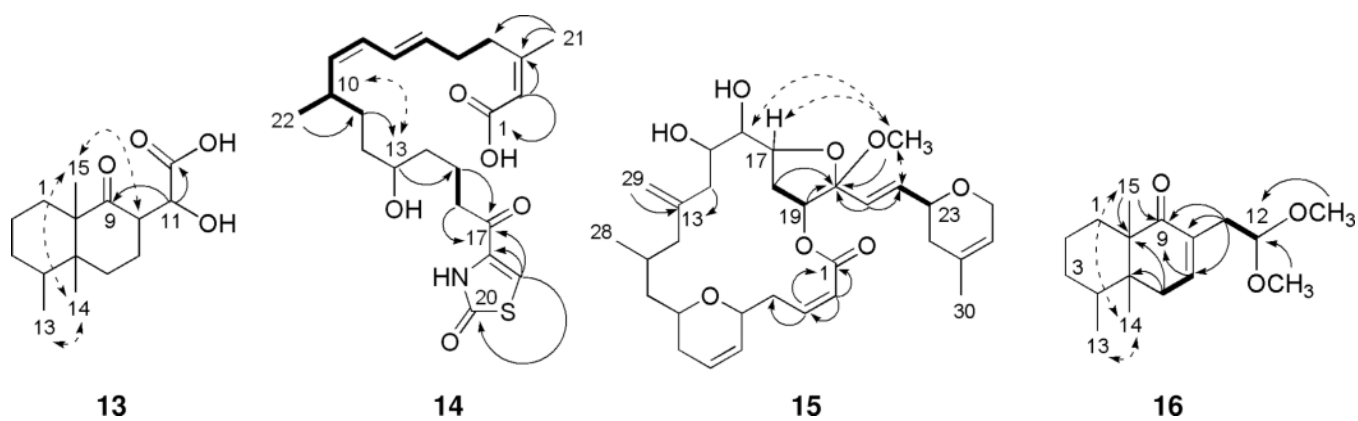
**Figure 1.**

One case example of an HT analysis to assess metabolite complexities of the constituents of a sponge extract from *C. mycofijiensis* (sample coded 07327 F XFD). Comparison of LC-MS-UV-ELSD data for: (a) the analytical trace and (b) the library trace representing dereplication of the constituents compounds 1–16 shown in Figure 2, based on interpretation of diagnostic *m/z* ions (in italics) and NMR data.

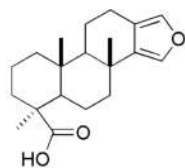
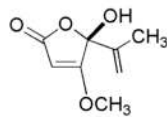
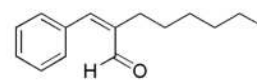


**Figure 2.** Compounds identified by LC-MS-UV-ELSD and NMR analysis of the library fractions shown in Figure 1, isolated from the extract of the sponge *C. mycofijiensis* (sample coded 07327 F XFD).

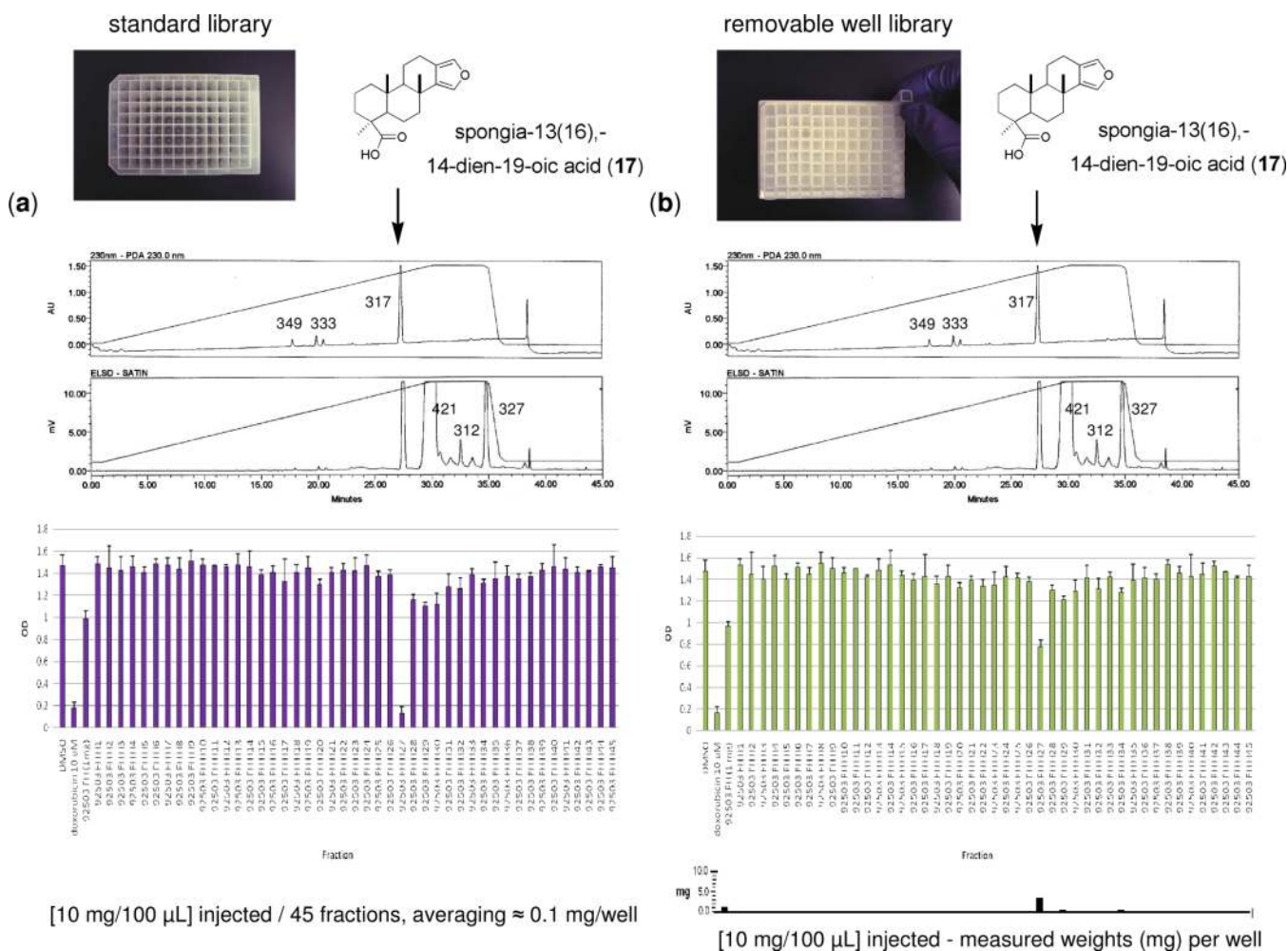




**Figure 3.** Selected 2D NMR results to establish carbon frameworks of new compounds present in the extract from *C. mycofijiensis* (sample coded 07327 F XFD) shown Figure 1b. These data consist of significant COSY (bold), HMBC (arrows), and NOESY (dashed) correlations observed for **13–16**.

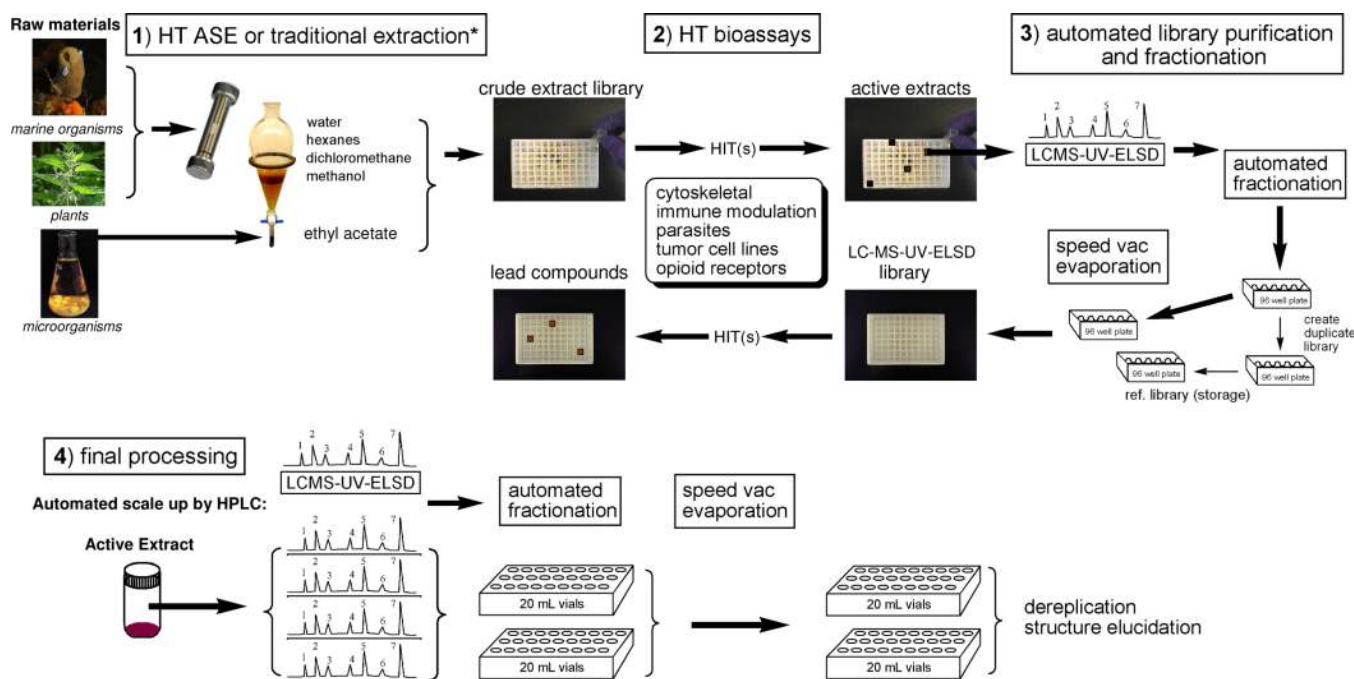
spongia- 13(16),-14-dien-19-oic acid (**17**)penicillic acid (**18**)hexylcinnamaldehyde (**19**)

**Figure 4.**  
Compounds identified as exhibiting bioactivity using the LC-MS-UV-ELSD library analysis of bioactive extract samples derived from a sponge and microorganisms.



**Figure 5.**

Assessing the quality of bioassay hits obtained from LC-MS-UV-ELSD libraries evaluated at a standard concentration of 10  $\mu$ g/mL. Contrasting two data sets obtained by two different approaches used to estimate metabolite concentrations in individual wells (standard vs removable 96 well plates). Comparative LC-MS-UV-ELSD traces with annotations of  $m/z$  ions (top) and cytotoxicity data (bottom) of coll. no. 92503, extract FH against macrophage (RAW 264.7) cells using an MTT bioassay with: (a) standard library consisting of dividing a 10 mg/100  $\mu$ L injection by 45 fixed wells to be at the average of  $\approx$  0.22 mg followed by generating a duplicate library (removing  $\frac{1}{2}$  the library volume with a 12 channel multipipeter) to arrive at an assumed  $\approx$  0.1 mg/well weight for both libraries and (b) removable well library with well fraction concentrations based on measured weights/well from a 10 mg/100  $\mu$ L injection.

**Scheme 1.**

High throughput (HT) flow of raw materials involving: **1)** extraction (accelerated solvent extraction, ASE), **2)** bioassays, **3)** automated library purification and fractionation and **4)** final processing using automated scale up HPLC to initiate dereplication or structure elucidation of lead compounds. \*Polyamide solid phase extraction (SPE) cartridges were used to remove polyphenols from MeOH plant extracts.

Illustrating the process of using a positive biological response from an extract of the sponge *C. mycofijiensis* (sample coded 07327 F XFD), to prepare an LC-MS-UV-ELSD library (Figure 1b) for pinpointing the compounds (Figure 2) responsible for the biological activities observed in the parent extract. The discovery path illustrated by these data involves: (a) evaluation of library fractions in 7 bioassays at 3 institutions, and (b) analysis of selected library fractions interpreting LC-MS  $m/z$  ion and NMR data to identify specific compounds.

Table 1

entry	library fraction <sup>d</sup>	Institution assay	UCSC LC-MS <sup>a</sup>	$m/z$	compound	UCSC MF <sup>b</sup>		UCSC MT <sup>c</sup>	UCSF <i>T. brucei</i>	EISAI MDA-MB-435	EISAI HT-29	EISAI H522-11	EISAI U937
						obs. activity	IC <sub>50</sub> µg/mL						
1	F XFD $\epsilon$	*	*			+	+	5.8	>0.8 – < 2.5	>0.8 – < 2.5	>0.8 – < 2.5	>0.8 – < 2.5	>0.8 – < 2.5
2	F XFD H20	438	latrunculol A (1)		+	+	0.09	>2.5	0.65	0.76	0.31	0.31	
3	F XFD H22	436	latrunculone A (2)		–	–	3.6	>2.5	>2.5	>2.5	>2.5	>2.5	
4	F XFD H28	434	latrunculol B (3)		+	–	2.0	>2.5	>2.5	>2.5	>2.5	>2.5	
5	F XFD H30	269	aignopsanoic acid B (13)		–	–	>10.0	>2.5	>2.5	>2.5	>2.5	>2.5	
6	F XFD H33	404	apo latrunculin T (14)		–	–	4.8	>2.5	>2.5	>2.5	>2.5	>2.5	
7	F XFD H37	460	latrunculone B (4)		+	–	1.0	>2.5	>0.8 – < 2.5	>0.8 – < 2.5	1.18	1.18	
8	F XFD H38	529	fijianolide D (5)		–	+	1.4	>2.5	>2.5	>2.5	>2.5	>2.5	
9	F XFD H44	251	aignopsanoic acid A (6)		–	–	6.5	>2.5	>2.5	>2.5	>2.5	>2.5	
10	F XFD H47	515	fijianolide B (8)		–	+	0.08	0.002	0.003	0.002	0.002	0.003	
11	F XFD H52	515	fijianolide A (9)		–	+	1.4	0.02	0.04	0.02	0.03	0.03	
12	F XFD H54	404	latrunculin A (10)		+	–	1.2	0.04	0.08	0.06	0.07	0.07	
13	F XFD H56	405	mycothiazole (11)		–	–	6.7	1.0	0.7	1.0	0.01	0.01	
14	F XFD H57	513	20-methoxy-fijianolide A (15)		–	+	>10.0	>2.5	>2.5	>2.5	>2.5	>2.5	
15	F XFD H59	265	methyl aignopsanoate (7)		–	–	>10.0	>2.5	>2.5	>2.5	>2.5	>2.5	
16	F XFD H61	249	aignopsane ketal (16)		–	–	>10.0	>2.5	>2.5	>2.5	>2.5	>2.5	
17	F XFD H65	463	sacrotride A (12)		–	–	>10.0	>2.5	>2.5	>2.5	>2.5	>2.5	

<sup>a</sup> Observed  $m/z$  ions in positive ion mode using ESI-TOF mass spectrometer.

<sup>b</sup> Microfilament (MF) disruption against HeLa cells: (+) active, (–) inactive at 20 µg/mL.

<sup>c</sup> Microtubule (MT) disruption against HeLa cells: (+) active, (–) inactive at 20 µg/mL.

<sup>d</sup> Library fractions were assayed assuming ~0.1 mg/well. This was based on averaging the amount of extract injected to create each library [15 mg/100 µL] divided by 70 fractions ≈ 0.2 mg/well and then factoring in a loss of 50% from the generation of a reference library.